Reactions of Charged Substrates. 5. The Solvolysis and Sodium Azide Substitution Reactions of Benzylpyridinium Ions in Deuterium Oxide

Neil Buckley* and Norman J. Oppenheimer*

The Department of Pharmaceutical Chemistry, S-926, Box 0446, The University of California, San Francisco, California 94143-0446

Received April 22, 1996[⊗]

Second-order rate constants and activation values were measured for the reactions with NaN_3 of a series of 4-Y-substituted (Y = MeO, Me, H, Cl, and NO_2) benzyl 3′-Z-substituted (Z = CN, $CONH_2$, H, F, Ac) pyridinium chlorides in deuterium oxide. 3′-Cyanopyridine substrates reacted much faster than nicotinamide and pyridine substrates; in the pyridine series the 4-Me, 4-H, and 4-Cl benzyl analogs did not react *for up to 6 months at 96 °C in 1.7 M* NaN_3. The 3′-cyanopyridine substrates do not exhibit borderline kinetic behavior, but the nicotinamide substrates do. The Hammett plot is flat for the NaN_3 reaction of 3′-cyanopyridine substrates and increasingly V-shaped for the nicotinamide and pyridine substrates. The values of β_{LG} (four-point plot) for the NaN_3 reaction of the 4-MeO benzyl substrates is −1.45, which is usually interpreted as being a very "late" activated complex. Two-point Brønsted "plots" for the other benzyl derivatives and for two *N*-methylpyridinium ions give values of β_{LG} in the same range. The second-order rate constant and activation values for *N*-methyl-3′-cyanopyridinium iodide are within the same range as those for the benzyl substrates. For the hydrolysis reaction, the Hammett plot is linear for 3′-cyanopyridine substrates ($\rho^+ = -1.24$) and flat for the nicotinamide substrates. The extent of hydrolysis of 0.005−0.05 M solutions of the 3′-cyanopyridinie substrates depended on the initial concentration of substrate, and hydrolysis was slowed significantly or stopped completely in the presence of exogenous 3-cyanopyridine. These results show that an equilibrium is established among the products for the 4-MeO, 4-Me, 4-H, and 4-Cl substrates; the 4-NO_2 substrate reacted too slowly to discern any difference. Data for the extent of hydrolysis were fitted by an equation derived assuming the equilibrium. Despite this limitation on a classic test of mechanism, the rates and ρ values are consistent with direct displacement by solvent and not with a unimolecular process. These results, which are rationalized in terms of the Pross−Shaik model, suggest that there are no ion−dipole complex intermediates in the benzyl series and show that borderline kinetic behavior is a function of leaving group ability and is not necessarily related to a change in mechanism. A computational approach was used to evaluate anomalous β_{LG} values for the hydrolysis and nucleophilic substitution reactions of the methypyridinium ion substrates. It was found that neither the Nu−substrate bond lengths nor the difference in charge matched the β_{LG} values. The value of $\Delta\Delta S^{\ddagger}$ of −15 gibbs/mol between (4-methoxybenzyl)-3′-cyanopyridinium chloride and the corresponding dimethylsulfonium chloride in the NaN_3 reaction, which is the result of the solvation of the pyridine at the transition state and the lack of solvation of SMe_2, is used to argue that the source of NAD^+ glycohydrolase "catalysis" of NAD^+ bond cleavage is the result of desolvation of the leaving group upon binding.

Introduction

Oppenheimer *et al.* have studied the cleavage of the nicotinamide−ribosyl bond in nicotinamide−adenosine dinucleotide (NAD^+)[1] and in a series of 2′-substituted β-nicotinamide ribosides[2] and arabinosides,[3] and Schuber and his colleagues have studied the solution and NAD^+ glycohydrolase (EC 3.2.2.6)-catalyzed cleavage of NAD^+ analogs with different pyridine leaving groups.[4] All the evidence suggests that bond cleavage is dissociative and involves either an S_N1 or an ion−dipole complex (designated IDC for solution reactions) mechanism. A purely dissociative mechanism is at odds with a suggestion made by Jencks[5] that sugar oxocarbenium ions are too unstable to exist as solvent-equilibrated intermediates or in contact with a strong nucleophile such as N_3^- in solution.

In a computational study of the gas-phase dissociation of β-nicotinamide riboside in the presence of several water molecules, Schröder *et al.*[6] found that the structures of the activated complexes and energies of the transition states for the inversion and retention reactions were different, which led them to question the general validity of the "exploded" transition state invoked by Sinnott and Jencks[7] to explain the relative reactivities and selectivities of glucosyl pyridinium ions. A recent study of the gas-phase dissociation of Handlon's series[2] of 2′-substituted β-nicotinamide arabinosides showed that dissociation occurred through an ion−neutral complex intermediate[8] (designated an INC for the gas-phase

* Address correspondence to N.B. as follows: Phone: (707) 824-9770. Fax: (415) 476-9687. E-mail: buckley@cgl.ucsf.edu.

⊗ Abstract published in *Advance ACS Abstracts,* September 15, 1996.

(1) Johnson, R. W.; Marschner, T. M.; Oppenheimer, N. J. *J. Am. Chem. Soc.* **1988**, *110*, 2257−2263.

(2) Handlon, A. L.; Oppenheimer, N. J. *J. Org. Chem.* **1991**, *56*, 5009−5010.

(3) Handlon, A. L.; Xu, C.; Müller-Steffner, H.-M.; Schuber, F.; Oppenheimer, N.J. *J. Am. Chem. Soc.* **1994**, *116*, 12087−12088.

(4) Tarnus, C.; Schuber, F. *Bioorg. Chem.* **1987**, *15*, 31−42. Tarnus, C.; Muller, H. M.; Schuber, F. *Ibid.* **1988**, *16*, 38−51.

(5) Young, P. R.; Jencks, W. P. *J. Am. Chem. Soc.* **1977**, *99*, 8238−8248. Amyes, T. L.; Jencks, W. P. *J. Am. Chem. Soc.* **1989**, *111*, 7888−7900. Banait, N. S.; Jencks, W. P. *J. Am. Chem. Soc.* **1991**, *113*, 7951−7958.

(6) Schröder, S.; Buckley, N.; Oppenheimer, N. J.; Kollman, P. A. *J. Am. Chem. Soc.* **1992**, *114*, 8232−8238.

(7) Sinnott, M. L.; Jencks, W. P. *J. Am. Chem. Soc.* **1980,** *102*, 2026−2032.

S0022-3263(96)00729-3 CCC: $12.00

reaction). Correlations among the measured relative rates and the AM1 values of $\Delta H^{\ddagger}$ for the gas-phase reaction and the experimentally determined values of $\Delta G^{\ddagger}$ for the solution reaction strongly suggested that the mechanism of dissociation was the same in both phases, but that the rate-limiting step was different.

It seemed that some insight into the question of intermediate stability and mechanism might be gained by studying the hydrolysis and nucleophilic substitution reactions of pyridinium ion substrates with potentially stable carbenium ion intermediates. Benzyl substrates provide a convenient system because the structure of both the putative intermediate and leaving group can be varied easily. It was established with certainty recently that the (4-methoxybenzyl)carbenium ion is an intermediate in the solvolysis and N_3^- substitution reactions of neutral (benzoates and chlorides[9]) and charged (dimethylsulfonium ion[10,11]) substrates. Other evidence[12] suggests that (4-substituted benzyl)dimethylsulfonium ions bearing substituents with $\sigma^+ > -0.31$ react with nucleophiles and water by direct displacement.

Katritzky[13] has published a large amount of data on the substitution reactions of benzyl and other substrates with highly arylated or fused-ring pyridines as the LG in chlorobenzene with neutral amine nucleophiles, primarily piperidine. (4-Methoxybenzyl)-2′,4′,6′-triphenylpyridinium ion and several of the fused-ring substrates exhibit borderline kinetics—k_{obsd} does not double with a doubling of the concentration of nucleophile—but benzyl triphenylpyridinium ion substrates bearing 4-Y-groups with $\sigma^+ > -0.31$ do not. The Hammett plot for the second-order reactions of all triphenylpyridinium ion substrates is linear (see below). Katritzky interpreted these results in terms of an IDC and not a mixed mechanism (Scheme 1).

We have prepared and studied the reaction with NaN_3 in D_2O of a series of (4-Y-benzyl)-3′-Z-substituted pyridinium chlorides (Chart 1). Because the rate constants could be measured conveniently, we have concentrated on **1a**−**e**. While most anionic nucleophiles add to the 2- or 4-position of pyridinium ions to give "dead-end" products that do not hydrolyze, N_3^- does not. Because of this limitation on the range of nucleophiles, we can obtain β_{LG} but not β_{Nuc}. Unlike Katritzky's results in chlorobenzene with neutral nucleophiles, we found that all substrates reacted with NaN_3 in a strictly second-order manner and that hydrolysis appears to occur by direct solvent displacement.

With Maltby and Burlingame, we measured the relative rates for the gas-phase dissociation of these pyridinium ion substrates and have reported the results elsewhere.[14] Thus, we have solution, gas-phase, and computational results, obtained in the same laboratory under essentially identical conditions, for the ribosyl and benzylpyridinium ions that can be compared directly. In brief, the comparison shows that the ribosyloxocarbenium ions are intrinsically more stable than the benzylcarbenium ions in the gas phase and that the mechanisms of hydrolysis and NaN_3 substitution are different, with unimolecular reactions for the ribosyl compounds and bimolecular reactions for the benzylpyridinium ions. (With our work on benzyldimethysulfonium ions, we have a system with which to compare the effects of the LG.) These results are inconsistent with the supposition that the ribosyl oxocarbenium ions cannot exist as discrete intermediates on the reaction coordinate for either solution or enzyme-catalyzed reactions.

Scheme 1

Ion-Dipole Complex Mechanism

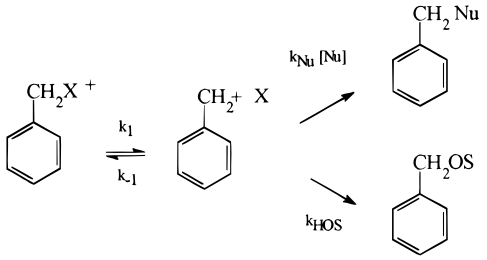

Mixed S_N1/S_N2 Mechanism

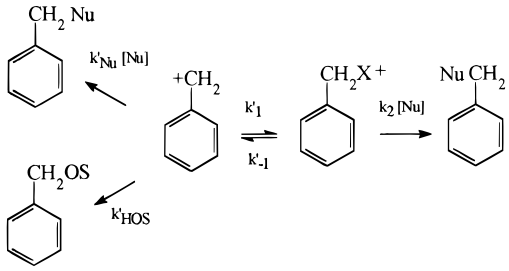

Chart 1

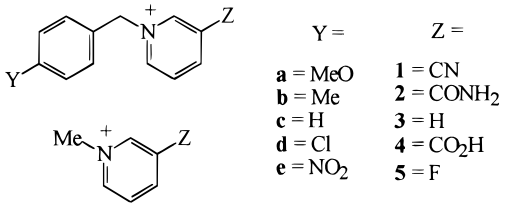

Experimental Section

General Procedures. All chemicals were obtained from Aldrich and used without further purification. NMR spectra were recorded on a General Electric QE-300 FT-NMR fitted with a variable-temperature probe rated at ±0.1 °C. Liquid secondary ion mass spectra (LSIMS) were obtained on a four-sector Kratos Concept II in the positive ion mode in the UCSF Mass Spectrometry Facility. Plots were made, and linear regression was performed on Origin V2.8 or 4.0.

Syntheses. All substrates were prepared by alkylation of the appropriate pyridine with the appropriate benzyl chloride using methods described elsewhere.[14] Nicotinamide and 3-cyanopyridine were alkylated with MeI using the same procedure. Appropriate ^1H and ^{13}C NMR and LSIMS spectra[14] were obtained for all compounds, which have been prepared previously as various salts (tosylates, triflates, iodides, etc.); they were not further characterized.

Kinetics. Two methods were used to obtain *pseudo*-first-order rate constants (k_{obsd}). For **2a**−**e** and **3a**−**e**, ca. 1−2 mM solutions were made up in NMR tubes with the appropriate NaN_3 stock solution in D_2O, with NaCl added to control ionic strength, and heated in thermostated heat blocks (sand bath) at 96 °C. The concentration of substrate was varied routinely and had no effect on k_{obsd}. Tubes were removed and spectra

(8) Buckley, N.; Handlon, A. L.; Maltby, D.; Burlingame, A. L.; Oppenheimer, N. J. *J. Org. Chem.* **1994**, *59*, 3609−3615.
(9) Amyes, T. L.; Richard, J. P. *J. Am. Chem. Soc.* **1990**, *112*, 9507−9512.
(10) Buckley, N.; Oppenheimer, N. J. *J. Org. Chem.* **1994**, *59*, 5717−5723.
(11) Kevill, D. N.; Ismail, N. H. J.; D'Souza, M. J. *J. Org. Chem.* **1994**, *59*, 6303−6312.
(12) Friedberger, M. P.; Thornton, E. R. *J. Am. Chem. Soc.* **1976**, *98*, 2861−2865.
(13) Reviewed in: Katritzky, A. R.; Brycki, B. E. *Chem. Soc. Rev.* **1990**, *19*, 83−105 and elsewhere.
(14) Buckley, N.; Maltby, D.; Burlingame, A. L.; Oppenheimer, N. J. *J. Org. Chem.* **1996**, *61*, 2753−2762.

recorded at approximately 22 h intervals. For **1a**−**e**, the appropriate stock solutions of NaN_3 in D_2O were heated in the probe of the NMR at various temperatures (40−90 °C), the tube was removed, substrate was added to make ca. 5−10 mM solutions, the tube was returned to the probe and shimmed after ca. 1 min to allow equilibration, and spectra were recorded at various time intervals. For particularly slow reactions—those that were complete within 4−5 h—tubes were held in thermostated heat blocks at the appropriate temperature and transferred at various intervals to the heated NMR probe in a round-robin fashion.

The 2′ and 6′ pyridine protons rapidly exchanged for all substrates under the reaction conditions. Depending on the substrate, the benzyl methylene protons would also exchange, slowest for the 4-MeO derivatives and fastest for the 4-NO_2 derivatives. Therefore, rate constants were determined by measuring the disappearance of the multiplet for the nonexchanging pyridine 5′ proton. The total substrate was taken as the sum of the substrate and product peaks, which provided an internally consistent standard. As a check on the method, in some instances the disappearance of the substrate benzyl aromatic AA′BB′ peaks or the 4′ pyridine peak was monitored; in all instances, the same rate constant was obtained.

The NaCl used to control ionic strength had no effect on the rates. For instance, plots of k_{obsd} vs [NaN_3] for **1a**−**e** extrapolate to 0 at 80 °C; if there is a reaction with Cl^-, it is very slow and k_{Cl^-} would not contribute significantly to k_{obsd}. For **1a-c**, **2a**−**e**, **1-Me**, and **2-Me**, hydrolysis at 96 °C in pure D_2O occurs faster than hydrolysis in 1.7M NaCl solutions, consistent with an effect of ionic strength on rate and not with a bimolecular reaction with Cl^-.

Product analysis was performed by extracting reaction mixtures with $CDCl_3$ and integrating the appropriate aromatic AA′BB′ peaks in ^{1}H-NMR spectra.

Suppression Studies. For studies of the suppression of hydrolysis in the absence of exogenous leaving group, serial dilutions were made of stock solutions of the appropriate pyridinium ion in D_2O. Aliquots in NMR tubes were heated in thermostated heat blocks (sand bath), and spectra were recorded at intervals of 1−2 days. For studies of suppression of hydrolysis with an exogenous leaving group for **1a**−**e**, 5 mM solutions of substrate containing 5 mM 3-cyanopyridine were heated and analyzed as described above.

Results

NaN_3 Kinetics. Values of *pseudo*-first-order k_{obsd} were obtained by linear regression as the slopes of plots of ln (C_t/C_o) vs time, where C_t was the relative concentration at time t measured from the 5′-pyridine peak and C_o was the sum of the relative concentrations of C_t and product pyridine. For **1a**−**e** and **1-Me**, plots were linear over three to four measured half-lives and generally had $r \geq 0.990$; in several instances the r values were in the range 0.980 to 0.990. For **2a**−**e, 3a,e, 5a,e**, and **2-Me**, plots were linear over 1−4 half-lives (see below). Values of k_{obsd} typically varied by 1−10% SE. Second-order rate constants (k_2) were determined by linear regression from plots of k_{obsd} vs [NaN_3] (Table 1). In all but two instances, $r \geq 0.996$. For **1a**−**e**, plots were based on the averages of two to eight determinations. For the much slower reactions of **2a**−**e**, **3a,e**, **5a,e**, and **2-Me**, plots were based on duplicate determinations of k_{obsd}.

Activation values for **1a**−**e** were determined from four- to five-point Eyring plots (range 50−90 °C) by linear regression ($r \geq 0.998$). For **1-Me** iodide, only three points were used (70−90 °C, $r = 0.9999$). Values summarized in Table 2 are reported ± SD.

(a) 3-Cyanopyridines. These substrates reacted smoothly with NaN_3 at convenient rates in the range 50-90 °C. Plots of k_{obsd} vs [NaN_3] were linear over more than half of the concentration of NaN_3, after which a slight curvature could be seen, especially for the plots at 70, 80, and 90 °C (Figure 1). Curvature is most probably the result of a negative primary salt effect expected for reaction between two oppositely charged ions. These plots appear to intercept the origin within error; as shown below, however, there is a slow hydrolysis reaction. Second-order rate constants for reaction at 80 °C (μ = 1.7, NaCl), determined in the range 0−1.7 M NaN_3 (all $r > 0.999$), are listed in Table 1.

Second-order rate constants for **1-Me** were determined at 70, 80, and 90 °C from plots of k_{obsd} vs [NaN_3] (0−1.7 M, $r > 0.996$). Unlike the benzyl substrates, however, there were non-zero intercepts for the second-order plots, with rate constants in the range 1.5×10^{-3} to 17×10^{-3} min^{-1} for the three temperatures. An extrapolation gives

Table 1. Second-Order Rate Constants for the Reaction of 1a−e (80 °C) and 2a−e (96 °C) with NaN_3 (k_2) and Water (k_w)[a]

Y	k_2 (min^{-1} M^{-1})	k_w (min^{-1} M^{-1})	k_{rel}
1a−e			
MeO	$9.6 \pm 0.09 \times 10^{-2}$	23.9×10^{-6}	0.4×10^4
Me	$10.4 \pm 0.4 \times 10^{-2}$	7.8×10^{-6}	1.3×10^4
H	$8.3 \pm 0.3 \times 10^{-2}$	3.1×10^{-6}	2.6×10^4
Cl	$11.2 \pm 0.5 \times 10^{-2}$	1.8×10^{-6}	6.2×10^4
NO_2	$9.1 \pm 0.3 \times 10^{-2}$	0.3×10^{-6}	36.0×10^4
1-Me	$7.5 \pm 0.2 \times 10^{-2}$	5.9×10^{-5}	0.14×10^4
2a−e			
MeO	$5.3 \pm 0.7 \times 10^{-4}$	2.2×10^{-6}	241
Me	$5.3 \pm 0.8 \times 10^{-4}$	2.3×10^{-6}	230
H	$2.9 \pm 0.1 \times 10^{-4}$	2.0×10^{-6}	145
Cl	$2.4 \pm 0.2 \times 10^{-4}$	2.5×10^{-6}	96
NO_2	$5.3 \pm 0.8 \times 10^{-4}$	2.0×10^{-6}	265
2-Me	$2.3 \pm 0.7 \times 10^{-4}$	1.6×10^{-6}	144

[a] All rate constants determined at $\mu = 1.7$ (NaCl). NaN_3 range 0−0.85M for **1a, 2a**−**e, 2-Me**; 0−1.7 M for **1b**−**e, 1-Me**. For **1a**−**e**, all $r \geq 0.999$; for **2a**−**e**, all $r \geq 0.980$. $k_w = k_{obsd}/55.5$. For **1a**−**e**, k_{obsd} for the water reaction was estimated from the plots in Figure 6; for **2a**−**e** and **2-Me**, k_{obsd} for the water reaction were measured directly (as in Figure 2).

Table 2. Eyring Activation Values for the Reaction of 1a−e and 1-Me with NaN_3[a]

Y	$\Delta H^{\ddagger}$ (kcal/mol)	$\Delta S^{\ddagger}$ (gibbs/mol)	$\Delta G^{\ddagger}_{80}$ (kcal/mol)	r
MeO	17.6 ± 0.8	-21.6 ± 2.0	25.2	0.9970
Me	15.7 ± 0.6	-26.9 ± 1.6	25.3	0.9980
H	14.4 ± 0.1	-30.9 ± 0.4	25.3	0.9999
Cl	15.6 ± 0.4	-28.8 ± 1.3	25.2	0.9992
NO2	14.8 ± 0.3	-29.7 ± 0.8	25.3	0.9995
1-Me	15.0 ± 0.1	-29.5 ± 0.2	25.8	0.9999

[a] Determined from four to five point plots for **1a**−**e** and a three-point plot for **1-Me**.

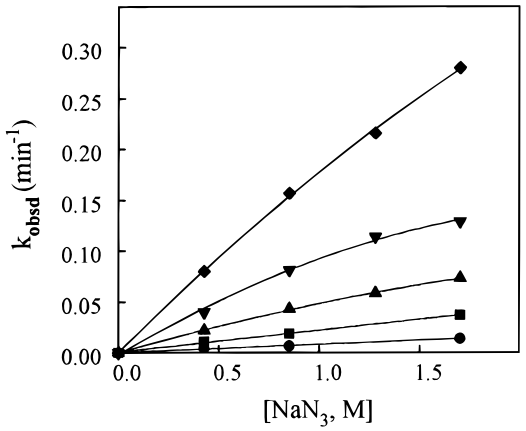

Figure 1. Second-order rate plots for the reaction of **1a** with NaN_3 (μ = 1.7, NaCl) in D_2O at 50 °C (●), 60 °C (■), 70 °C (▲), 80 °C (▼), and 90 °C (◆).

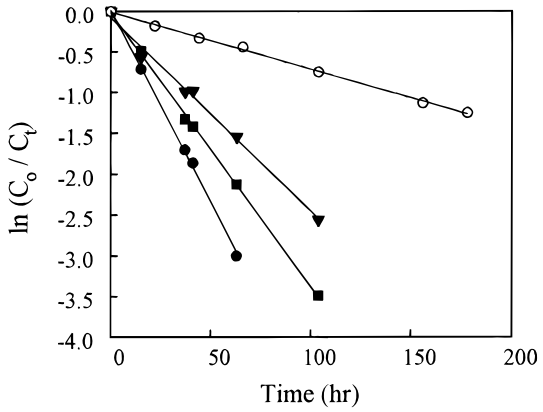

Figure 2. Rate plots for the reaction of **2a** with NaN_3 (μ = 1.7, NaCl) in D_2O at 96 °C. [NaN_3] = 1.7 (●), 0.85 (■), 0.43 (▲); ○ = water only. The *r* values are 0.9994, 0.9995, 0.9962, and 0.9992, respectively.

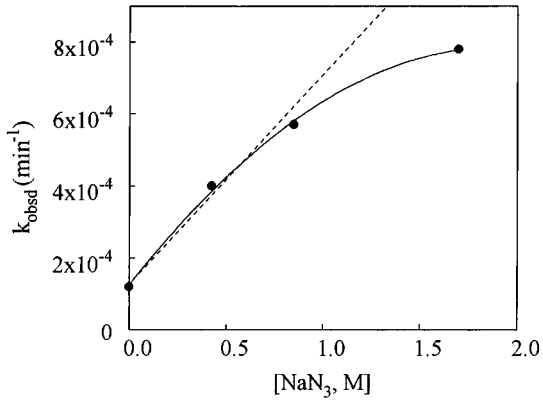

Figure 3. Second-order rate plot for the reaction of **2a** with NaN_3 (μ = 1.7, NaCl) in D_2O at 96 °C. The dashed line is a regression fit (*r* = 0.990) to the point for water alone and 0.43 M and 0.85 M NaN_3.

a value of ca. 40 × 10^{-3} min^{-1}, or k_w = 7.2 × 10^{-4} M^{-1} min^{-1}, for the second-order rate constant at 96 °C.

(b) Nicotinamides. Rate plots for reaction of NaN_3 with **2a**−**e** were linear over 2−4 half-lives at 96 °C (Figure 2). Plots of k_{obsd} vs [NaN_3] are linear between 0 and 0.85 M NaN_3, after which curvature appeared in some plots (Figure 3). Curvature could be the result of the negative primary salt effect or it could be the result of NaN_3-catalyzed hydrolysis of the amide; because the pK_a for nicotinic acid is higher than that for nicotinamide, the displacement reactions would be slower and could account for the curvature. These plots had non-zero intercepts (k_{hyd}), and there was a measurable reaction in water alone; the rate constants were the same within error. Values for the second-order rate constants were taken from the linear portions of the curves (three points); these and the values for k_w, which for comparison with the NaN_3 numbers are the second-order rate constants k_{hyd}/55.5, are listed in Table 1.

(c) Pyridines. **3a** and **3e** reacted very slowly with NaN_3 at 96 °C. Second-order rate constants, based on 1−2 half-life k_{obsd} values, are listed in Table 1. For **3b**−**d**, however, *there was no detectable reaction at 96 °C in up to 1.7 M* NaN_3 *for 6 months!*

D_2O Only Kinetics. (a) 3′-Cyanopyridines. In D_2O alone, the extent of reaction is a function of the concentration of substrate. Shown in Figure 4 are plots of ln (C_o/C_t) vs time for the hydrolysis of 5−50 mM solutions of **1a** and **1b** at 80 °C; a similar pattern was found for

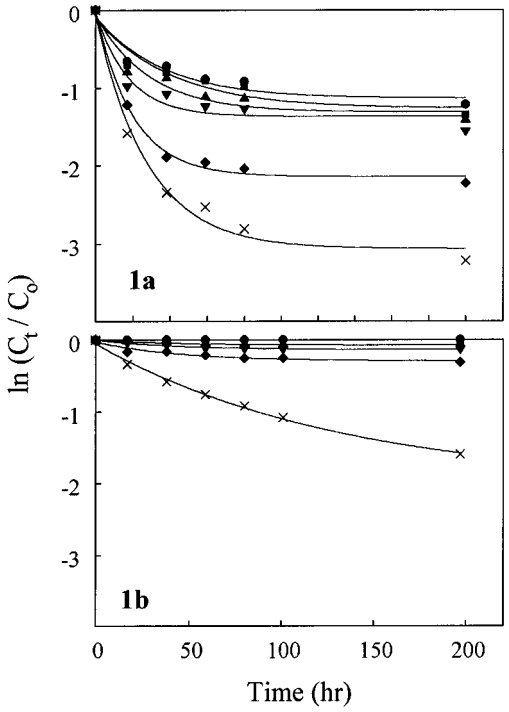

Figure 4. Reaction progress for **1a,b** at 80 °C in pure D_2O as a function of the initial molar concentration of substrate: 0.005 = ×; 0.010 = ◆; 0.020 = ▼; 0.030 = ▲; 0.040 = ■; 0.050 = ●.

the slower reactions of **1c-e** at 96 °C (5, 20, and 50 mM solutions; not shown). This curvature is the same as found for (4-methoxybenzyl)dimethylsulfonium chloride that we have shown[10] is caused by the establishment of the equilibrium $RX^+ \rightleftharpoons ROH + H_3O^+ + X°$ during the course of the reaction. For the sulfonium ions, data were fitted to a cubic equation derived for the equilibrium that assumed X° is not protonated, which is a reasonable assumption for SMe_2 (pK_a = −6). For pyridinium ions, however, a significant proportion of the liberated 3-cyanopyridine (pK_a = 1.45) would be protonated. With the simplifying assumption that [ROH] ∼ [XH^+], the equation for the equilibrium is

$$C_o = K_a K_{eq} f/(1 - f)^2$$

where C_o is the initial concentration of substrate, K_a is the acidity constant for the pyridine, K_{eq} is the equilibrium constant, and *f* is the fraction remaining at equilibrium ([RX^+]$_{200h}$/C_o). The fit of data for **1a** to this equation (C_o = 5−50 mM at *t* = 200 h) by the Marquand−Leverberger nonlinear least-squares algorithm in the Origin software is shown in Figure 5 (K_{eq} = 2.29 ± 0.06, χ^2 = 3.84 × 10^{-6}).

Studies of exogenous LG were limited for sulfonium ions by the solubility of SMe_2 in water.[10] Solubility of the pyridine LGs is not a problem, but it is difficult to analyze and quantitate the aromatic region of spectra containing large amounts of exogenous pyridine; for **1a** and **1b**, however, the methyl signals can be followed conveniently, and the same is true for the methylene signals for **1c** and **1d**, although for high concentrations of pyridines some exchange of these protons takes place and the readings can be inaccurate. Shown in Figure 6 are plots of ln (C_o/C_t) for the hydrolysis of 5mM solutions of **1a**−**d** in the presence of 5 mM 3-cyanopyridine (closed circles) at 80 °C; for comparison, the plots for 5 mM substrate alone are included (open circles). The presence of exogenous leaving group further suppresses the reaction.

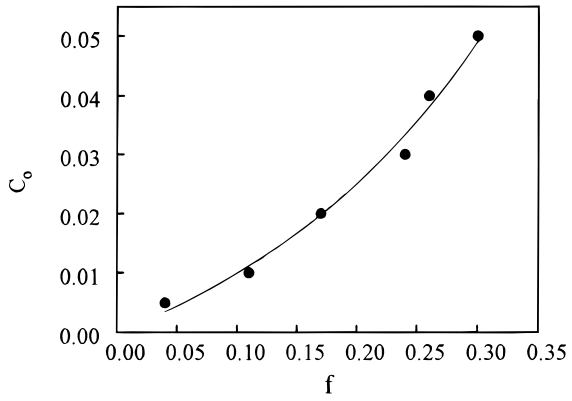

Figure 5. Fit of the data for **1a** from Figure 4 to the equation for the equilibrium $RPy^+ \leftrightarrows ROH + Py + H_3O^+$ D PyH^+. $K_{eq} = 2.29 \pm 0.06$, $\chi^2 = 3.8 \times 10^{-6}$.

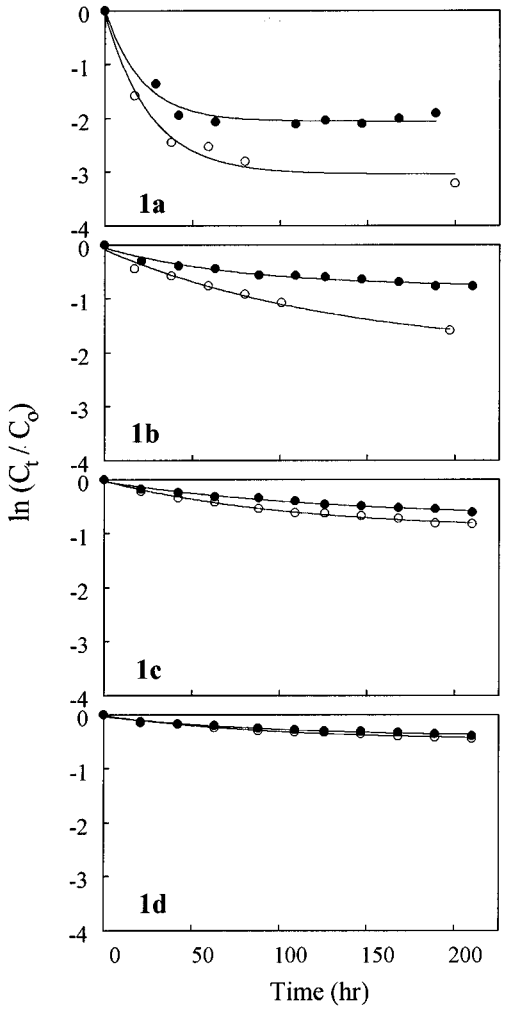

Figure 6. Reaction progress for 0.005M **1a**−**d** at 80 °C in pure D_2O with 0.005 M 3-cyanopyridine added (●) and in pure D_2O (○).

Because of the severe curvature and the fact that use of either the Guggenheim method or inclusion of an infinity value in the rate equation failed to give linear plots, it was difficult to obtain accurate values for the hydrolysis rate constants k_w. Points taken during the first half-life give approximately linear rate plots, however, and the values of k_w can be estimated. These are listed in Table 1.

NMR spectra for **1e** are very difficult to analyze because the benzyl methylene protons exchange rapidly under the reaction conditions, and the pyridinium ion and aromatic protons cannot be resolved well from those for product pyridine or alcohol. Nonetheless, spectra for 5, 30, and 50 mM solutions and 5 mM substrate plus 5 mM 3-cyanopyridine change only very slowly and to the same extent (measured by noting the change in the relative heights of the substrate and product 5′-proton, which is difficult to quantitate with any accuracy). We did not attempt to characterize this reaction further.

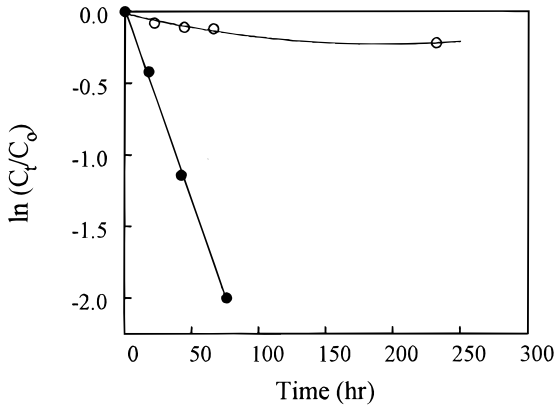

Figure 7. Rate plots for hydrolysis of **2a** (almost certainly hydrolyzed to the 3′-carboxy compound **4a**) in 5.3 M DCl at 80 °C (●), conditions that would prevent the equilibrium among starting material and products. The plot is linear ($r = 0.999$) over >3 half-lives. For reference, the hydrolysis of 0.005 M **4a** at 80 °C in pure D_2O is shown (○).

(b) Nicotinamide. The same concentration dependence found for the 3′-cyanopyridine substrates was seen for the nicotinamide substrates at 96 °C; the reaction was slower, and the extent of reaction was less than for **1a**−**e** (not shown). We did not repeat the reaction in the presence of nicotinamide.

In the (4-methoxybenzyl)dimethysulfonium ion work, we showed that if SMe_2 were removed as the Hg^{+2} or Zn^{+2} complexes, the reaction went to completion with no suppression.[10] In 5.3 M DCl at 96 °C, the amide moiety of nicotinamide would be hydrolyzed rapidly to the acid, and all nicotinic acid released by solvolysis would be protonated and the equilibrium with starting material would be suppressed; it is also probable that the bis benzyl ether, which would have essentially the same NMR spectrum as the alcohol, would form under these extremely acidic conditions, which would further suppress the equilibrium.[12] In the event, solvolysis of **2a** in 5.3 M DCl at 96 °C proceeded smoothly, and the plot of ln (C_t/C_o) vs time was linear over 3 half-lives (Figure 7; $r = 0.999$). Similar plots were obtained for hydrolysis in the presence of 2 M D_2SO_4 (not shown). For comparison, the rate plot for the same concentration of **4a**, which was prepared by saponification of the methyl ester, in D_2O ($\mu = 1.7$, NaCl) is shown in Figure 7; the estimated rate constant in DCl is 35-fold higher than in D_2O alone, and the plot for D_2O alone is slightly curved.

(c) Other Derivatives. The same concentration-dependent pattern was found for hydrolysis of **5a** and **6a** (plots not shown). Thus, the equilibrium among starting material and products is independent of the pK_a of the leaving group and is general for the class.

Linear Free Energy Relations (LFERs). (a) Hammett Plots. Hammett plots for the NaN_3 reaction of **1a**−**e** (80 °C), **2a**−**e** (96 °C), and **3a,e** (96 °C) are shown in Figure 8. For **1a**−**e**, the plot is flat. (Hammett plots based on k_2 values for lower temperatures show small increases to a V-shaped curve with decreasing temper-

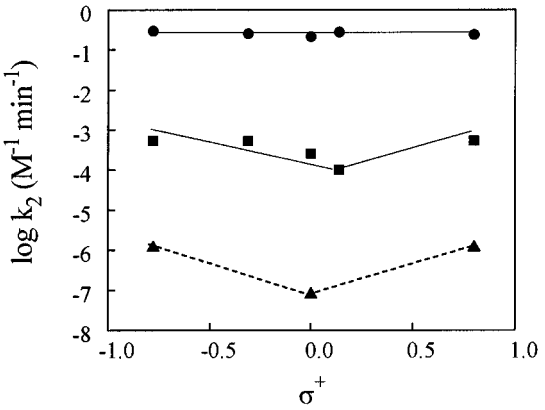

Figure 8. Hammett plots for the reaction with NaN_3 (k_2) of **1a**−**e** (●), **2a**−**e** (■), and **3a,e** (▲) (μ = 1.7, NaCl). The point for **3c** was estimated as described in the text.

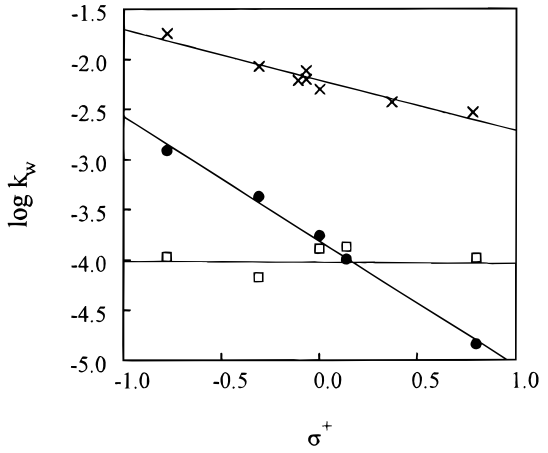

Figure 9. Hammett plots for the hydrolysis in D_2O of **1a**−**e** (●) and **2a**−**e** (□) at 80 and 96 °C respectively (μ = 1.7, NaCl). For **1a**−**e**, $\rho+ = -1.24$ (r = 0.997); for **2a**−**e**, $\rho+ = 0.05$ (r = 0.26). For reference, the Hammett plot is shown for Katritzky's second-order rate constants[13] for the reaction of benzyl triphenylpyridinium ions with piperidine in chlorobenzene at 100 °C (×); $\rho+ = -0.51$ (r = 0.960).

ature. The change is not great, however). For **2a**−**e**, the plot is V-shaped with the break at **2c**. As noted above, **3b**−**d** did not react with NaN_3 after 6 months at 96 °C; if it is assumed, however, that 3% reaction—the limit of NMR detection—had occurred for **3c**, the three-point plot in Figure 8 is obtained. This estimated point is the upper limit for k_2; it is entirely possible that the "real" value would be lower, and the break would be deeper. The salient feature is that with increasing basicity of the LG, the depth of the break in the Hammett plots increases.

The Hammett plot for the hydrolysis of **1a**−**e** (Figure 9), which is based on estimated rate constants, is linear, which indicates the same mechanism of hydrolysis for all substrates. For (4-methoxybenzyl)dimethylsulfonium chloride, the rates of hydrolysis and second-order reaction with NaN_3 are within the same range, and we have shown[10] that there is a change in mechanism from S_N1 for the (4-methoxybenzyl)dimethylsulfonium compound to S_N2 for substrates with less electron-donating 4-substituents, which react by direct displacement by solvent. Because of the great difference between the hydrolysis and NaN_3 second-order rate constants for **1a**−**e**, we assume that hydrolysis takes place by direct solvent displacement. The standard test for this, common leaving group suppression, cannot be applied here because of the equilibrium among products and starting materials, so our assignment of mechanism is of necessity circumstantial. The Hammett plot for hydrolysis of **2a**−**e** (Figure 9), based on directly measured rate constants, is essentially flat.

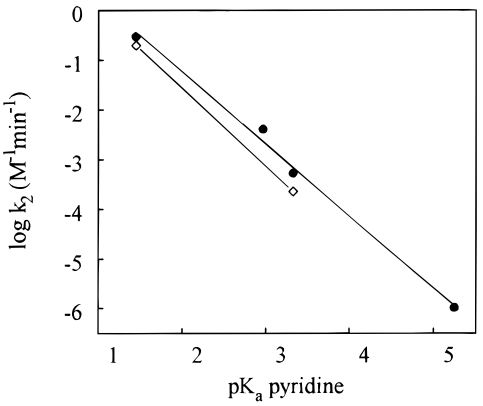

Figure 10. Brønsted plot for the NaN_3 reaction of (4-methoxybenzyl)pyridinium ions at 80 °C (μ = 1.7, NaCl) (●); $\beta_{LG} = -1.45$ (r = 0.997). Data for the reactions of *N*-methylpyridinium ions **1-Me** and **2-Me** with NaN_3 under identical conditions are shown (◇); $\beta_{LG} = -1.56$.

(b) Brønsted Plots. Values of β_{LG} at 96 °C were determined from plots of log k_2 vs pK_a of the pyridine for **1**−**3a** and **5a** and for **1-Me** and **2-Me**. Values of k_2 used in these plots were based on at least duplicate determinations; the second-order rate constants at 96 °C for the **1a** and **1-Me** were obtained from extrapolation of the Eyring plots. The Brønsted plot for **1**−**3a** and **5a** (Figure 10) is linear with $\beta_{LG} = -1.47$. The two-point "plot" for **1-Me** and **2-Me** (Figure 10) has a slope of −1.56; two-point "plots" for **2b**−**d** and **3b**−**d** (not shown) are parallel to the four-point line for **1**−**3a** and **5a**. (The Hammett plot (vs σ_m) for the effect of substituents on the pyridine in **1a** is linear [not shown; r = 0.991] with ρ = 8.9.)

For the hydrolysis reactions, rate constants determined for **1a-c** at 96 °C in single experiments were within factors of 2−4 of the rate constants for **2a**−**c**, and were subject to the uncertainties noted above. These give approximate β_{LG} values in the range −0.15 to −0.30. For **1-Me** and **2-Me**, however, the value of β_{LG} calculated from the rate constants based on the intercept values for **1-Me** NaN_3 second-order plots and the directly measured value for **2-Me** is −1.4, on the same order as the NaN_3 value.

Product Studies. The only product detected in NMR spectra of $CDCl_3$ extracts of reaction mixtures of **1a**−**e** was the corresponding benzyl azide. For **2a**−**e**, ∼5−10% of the respective alcohol could be detected, which is consistent with the concomitant hydrolysis reaction; the majority of the product was the respective benzyl azide. No alcohol was found for **3a** and **3e**, but because of the slow rate, these reactions were not taken to completion.

Discussion

Borderline kinetics in the substitution reactions of benzyldimethylsulfonium ions with NaN_3 in water[15] and for reactions of benzylpyridinium ions with neutral amines in chlorobenzene[13] have been interpreted in terms of an IDC mechanism; in both cases a mixed S_N1/S_N2 mechanism was rejected for various reasons (Scheme 1).

(15) Sneen, R. A.; Felt, G. R.; Dickason, W. C. *J. Am. Chem. Soc.* **1973**, *95*, 638−639.

Borderline kinetics in the reactions of *N*-(methoxymethyl)-*N*,*N*-dimethylanilinium ions with nucleophiles, however, was interpreted by Knier and Jencks[16] as evidence for a concerted mechanism that is "enforced" because the putative cationic intermediate in an IDC or stepwise mechanism, $MeO{=}CH_2^+$, was judged to be too unstable to exist as a distinct, solvent-equilibrated species. Using semiempirical methods we have recently examined the gas-phase dissociation of a number of compounds with a variety of oxocarbenium ion intermediates that can form by dissociation of different LGs (NMe_2Ar, Py, H_2O, MeOH, Me_2O)[17] and found that neither $MeOCH_2NMe_2Ar^+$ nor $MeOCH_2Py^+$ had a distinct transition state in either PM3 or AM1, consistent with the arguments of Knier and Jencks.[16] Sulfur-containing linear primary systems such as $MeSCH_2NMe_2Ar^+$ and secondary linear systems such as $MeOCHMeNMe_2Ar^+$- and $MeSCHMeNMe_2Ar^+$ and the respective pyridinium ions, protonated hemiacetals, methyl acetals, and dimethyloxonium ions gave distinct transtion states, however, with the INCs much more stable for the α-sulfur than for the α-oxygen compounds.[17] These results show an LG and substituent dependence that is not consistent with the general view on oxocarbenium ion stability.[18]

An often unstated assumption is that a substitution reaction must occur through a single mechanism; in Jencks's reviews on these matters,[18] the case is always cast in terms of *either* a stepwise or concerted mechanism. The last sentence of the Knier−Jencks paper[16] states the consequences of this assumption most boldly: "[A]ll solvolysis and substitution reactions at saturated carbon that proceed through S_N2 displacement mechanisms do so simply because the intermediate in *the alternative* S_N1 mechanism is too unstable to exist [italics added]." It seems reasonable, however, that if $\Delta G^{\ddagger}$ of competing uni- and bimolecular mechanisms are of the same magnitude, there is no reason why simultaneous stepwise and concerted reactions with nucleophiles cannot occur, as found recently for neutral[9] and charged[10,11] 4-methoxybenzyl substrates. It seems equally true that there is no reason to believe that an S_N1 reaction *must* occur for a substrate that contains an excellent incipient carbenium ion (as in **1**−**5a**). Furthermore, borderline kinetics do not necessarily have to signal the presence of borderline *mechanisms* involving solvolytically generated ion-pair intermediates or some intermediate (as opposed to direct) solvent nucleophilic participation.

Our results show that borderline kinetic behavior is variable across a series of substrates in which only minor structural changes are made in the LG at some distance from the reaction center. There is no borderline behavior in the reaction of **1a**−**e** with NaN_3 in water at 80 °C (Figure 1 for **1a**). A slow reaction with water can be measured for **1a**−**e**, however. The relative rates for the second-order reactions k_{Az}/k_w, where k_w is k_{obsd} for the water reaction/55.5, range from 4×10^3 for **1a** to 3.6×10^5 for **1e** (Table 1). While we cannot rule out an S_N1 reaction with absolute certainty because of the equilibrium among products and starting material (see Results), the much slower hydrolysis reaction is consistent with solvent displacement on **1a**−**e**. Moreover, if an IDC were an intermediate in the pyridinium ion reactions, it would be expected that an alcohol would be formed by attack of solvent on the intrinsically unstable IDC, but no alcohol products were detected for any 3′-cyanopyridine substrate.

For the nicotinamide substrates **2a**−**e**, there is borderline behavior at 96 °C. The rates of the NaN_3 and hydrolysis reactions for **2a**−**e** are comparable, as shown by the rate plots for **2a** in Figure 2; the ratios of the second-order rate constants k_{Az}/k_w are between 96 and 265, which is relatively constant and much lower than the range found for **1a**−**e**. Alcohol products are also found in the NaN_3 reaction of the nicotinamide substrates. This pattern of reactivity suggests that in these systems the switch from no borderline to borderline behavior is related to factors other than a change in mechanism. The analysis presented below suggests that in this system, at least, borderline kinetics is related to the LG ability and to the different effects of charged or neutral nucleophiles on the structure of the activated complex for an uncomplicated concerted displacement reaction.

LFER Correlations. The Hammett plots for the NaN_3 reaction show that the effect of the 4-substituents on the rate constants depends on the LG. The plot for **1a**−**e** is essentially flat, and the plot for **2a**−**e** is slightly V-shaped; the value of ρ for **2a**−**d** is ca. −0.7 (Figure 8). For the pyridine series, with the point for **3c** based on an estimated upper limit for the rate constant (see Results), the Hammett plot is even more V-shaped. The value of β_{LG} for the 4-methoxybenzyl substrates is −1.45 (Figure 10), and the Hammett plot based on σ_m values for the pyridine 3′-substituents is also quite large (+8.9, $r = 0.991$, not shown). Values for the other substituted benzyl substrates, based on more limited rate data, are in the same range. Therefore, the activated complex for the NaN_3 reaction is very "late" for all substituents.

Westaway and Ali[19] have shown that a change from a better to a worse leaving group (for the reaction of thiophenoxides with substituted *N*-benzyl-*N*,*N*-dimethylanilinium ions in DMF, a system in which the LGs have the same pK_a range as the pyridines used here) "loosens" the Nu−benzyl methylene bond with little effect on the benzyl methylene−LG bond. Kurz and El-Nasr[20] found the same effect in k_{14}/k_{15} ratios for the reactions of various pyridines with neutral MeX derivatives (X = I^-, ^-OTs, and ^-OTf). This "anti-Hammond" effect is present in our system as well. For the NaN_3 reaction, the tightness of the Nu−benzyl methylene bond in the activated complex would be expected to decrease as a function of the LG in the order **1** > **2** > **3**. The extent of substituent interaction with the reaction center would be expressed in the same order: The more fully formed the Nu−benzyl methylene bond, the less charge at the reaction center and the less conjugation to the substituents, which is the trend seen in the Hammett plots. While this is not a direct resonance interaction as found in α-MeO- or α-N_3- substituted benzyl systems, the decreased resonance interaction of 4-substituents on the phenyl ring with the reaction center is the same as that described recently by Richard et al.[21] Thus, stabilization of the activated complex is related more to the nucleophile−carbenium ion interaction, which is mediated by the pK_a of the LG, than to the relatively constant LG−carbenium ion interaction.

(16) Knier, B. L.; Jencks, W. P. *J. Am. Chem. Soc.* **1980**, *102*, 6789−6796.
(17) Buckley, N.; Oppenheimer, N. J. *J. Org. Chem.*, in press.
(18) Jencks, W. P. *Acc. Chem. Res.* **1980,** *13*, 161−169. Jencks, W. P. *Chem. Soc. Rev.* **1981**, *10*, 345−375.
(19) Westaway, K. C.; Ali, S. F. *Can. J. Chem.* **1979**, *57*, 1354−1367.
(20) Kurz, J. L.; El-Nasr, M. M. *J. Am. Chem. Soc.* **1982**, *104*, 5823−5824.
(21) Richard, J. P.; Amyes, T. L.; Jagannadham, V.; Lee, Y.-G.; Rice, D. J. *J. Am. Chem. Soc.* **1995**, *117*, 5198−5205.

This qualitative description of the effects of nucleophile, LG, and substituents on the activated complex is in complete accord with the Pross−Shaik[22,23] avoided crossing model. Of the four canonical configurations for the NaN_3 reaction, the form corresponding to product, Nu··R :X°, is clearly the more important for a tight Nu−benzyl bond (as in **1a**−**e**). As this bond is "loosened" with a change to a worse LG, the forms Nu:$^-$R$^+$:X° and Nu· R:$^-$ ·X° become more important; the effects of electron-donating substituents would be expressed in stabilization of R^+ in the former and would decrease in the normal manner, while an electron-withdrawing group would stabilize the latter, and accordingly the rate of the 4-NO_2 substrate is increased relative to H (as in **2a**−**e** and **3a,e**). There is also a direct LG effect that is independent of the effect on the nucleophile interaction with the reaction center. Addition of electron-withdrawing substituents to the pyridine improves the LG ability by lowering the pK_a and increases the ionization potential of the LG, which makes Nu· R:$^-$ ·X° less important for transition state mixing. The "tightening" effect on the nucleophile-carbenium ion center for a better LG and the effect of the LG on the stabilization of the canonical forms lead to a flattening of the Hammett plot for **1a**−**e** (Figure 8). Thus, our results are in complete accord with Pross's rationale for the shape of Hammett plots for benzyl substrates.[23]

The Hammett plots for the hydrolysis reaction of **1a**−**e** and **2a**−**e** show trends opposite those found for the NaN_3 reaction (Figure 9). The linearity of the plots for **1a**−**e** and **2a**−**e** indicates a single mechanism, and our assumption of reaction through solvent displacement is consistent with the ρ value of −1.24 for **1a**−**e**. The Hammett plot for the hydrolysis of **2a**−**e** is essentially flat. Thus, while there is no indication of a change in mechanism, it is clear that substituent effects as a function of the LG are expressed differently for a neutral than for a negative nucleophile. While we did not measure the rate constants for the hydrolysis of all benzyl substrates at 96 °C, second-order rate constants for **1c,d** (ca. $6-10 \times 10^{-6}$ M^{-1} min^{-1}) are within factors of 3−5 of the second-order rate constants for **2c,d**, which suggests that the value of β_{LG} for the hydrolysis reaction would be low (ca. −0.15 to −0.30 based on the approximate relative rates.)

For the reaction of a neutral nucleophile, the most important canonical form for the activated complex is Nu:° R^+ :X°. Because the neutral nucleophile would not interact with the reaction center as strongly as a negatively charged species, the bond length should remain relatively constant with a change in LG. The more basic LG would stabilize R^+, and in a "tight" activated complex for both the nucleophile and LG this interaction may lessen or even eliminate the effects of substituents, which is the trend found: the Hammett plot is flat for the more basic pyridine LG (Figure 9), and the β_{LG} is low ("tight").

There is a caveat, however. The β_{LG} values for the NaN_3 reaction for methyl and benzyl substrates are essentially the same (Figure 10), but the trend for the hydrolysis reaction is reversed, with β_{LG} −0.3 for the benzyls and $\beta_{LG} = -1.4$ for **1Me** and **2Me**. While results such as these may be rationalized, as Pross has suggested,[22] by differences between a two-form mix for Me substrates vs a three (or more)-form mix for substrates that can stabilize the activated complex by resonance (as benzyl and $MeOCH_2$− substrates may do), this does not appear to be the entire—or even correct—story.

Sufficient data are not available for the benzylpyridinium ions to permit analysis. There are enough data, however, from the work reported here and by Arnett and Reich[24] and Metzger's group[25] for $MePy^+$, and from Knier and Jencks[16] for $MeOCH_2$-NMe_2Ar^+ substrates, to analyze the effect of the LG on reaction with a range of negative and neutral nucleophiles, including water. The stability of the activated complex is a function of the interaction of both the LG and the Nu with the reaction center, and stability should be reflected in some measure of the rate.

β_{LG}'s for the Me substrates cover a wide range (−0.4 to −1.5) and appear to be independent of the charge on the nucleophile. Values for the $MeOCH_2$− substrates[16] are in a much narrower range (−0.54 to −0.9) and also appear to be independent of the charge on the nucleophile. The interaction of the Nu and LG with the reaction site can be evaluated with cross-correlation plots[26] of β_{LG} vs the Swain−Scott n_{MeI} value for the reactions of $MePy's^+$ with N_3^-, I^-, Ph_3P, and water,[27] and for $MeOCH_2$-NMe_2Ar^+ with HO^-, AcO^-, three primary amines, and water.[16] While these plots are generally used to evaluate the effect of a change in a substituent on a general acid or on a substrate, in principle there is no reason why they cannot be used to evaluate the equivalent effect for changes in the reactivity of nucleophiles and LGs.

For the various nucleophiles these plots show, in each case, a good linear relation for all nucleophiles except water, the points for which are significantly off the correlation lines (Figure 11). The slope of these plots is a measure of the sensitivity of the substrate to the nucleophile and is smaller for the $MeOCH_2$−substrate (0.13) than for the Me (0.43), or "earlier" for the stabilized substrate. Even though it might be argued that the point for $MeOCH_2NMe_2Ar^+$ is off the line because the hydrolysis of this substrate is stepwise with the formation of an oxocarbenium ion too unstable to exist outside the initial solvation shell—an argument made recently by Banait and Jencks[28] for the fate of the glycosyl oxocarbenium ion in the hydrolysis of α-fluoroglucose—and thus represents a change in mechanism, this is certainly not true for the methyl compounds. The data for both substrates are quite consistent with direct solvent displacement.

It seemed that an answer to this question could be obtained using computational methods. Complete energy surfaces were calculated in AM1[29] for the reactions

$$X^{\circ/-} + \text{R-3-CNPy}^+ \rightleftharpoons XMe^{+/o} + \text{3-CNPy}$$

for R = Me (**1Me**) and R = $MeOCH_2$− with the same

(22) Pross, A. *Adv. Phys. Org. Chem.* **1985**, *21*, 99−196.
(23) Pross, A.; Shaik, S. S. *Acc. Chem. Res.* **1983**, *16*, 363−370.

(24) Arnett, E. M.; Reich, R. *J. Am. Chem. Soc.* **1980**, *102*, 5892−5902.
(25) Berg, U.; Gallo, R.; Metzger, J. *J. Org. Chem.* **1976**, *41*, 2621−2624.
(26) Jencks, D. A.; Jencks, W. P. *J. Am. Chem. Soc.* **1977**, *99*, 7948−7960.
(27) Data for MePy's were obtained in different solvents at different temperatures; while these conditions affect the absolute rates, they should not affect the Brønsted coefficients. As shown in Figure 9 of ref 24, plots of log k vs pK_a for the Menschutkin reaction of pyridines with a variety of electrophiles in solvents that span the range from DMSO to water to nitrobenzene and nitroalkanes over a rate range of 10^9 (!) all have essentially the same slopes. Microscopic reversibility requires that the same is true for the reverse reaction.
(28) Banait, N. S.; Jencks, W. P. *J. Am. Chem. Soc.* **1991**, *113*, 7951−7958.

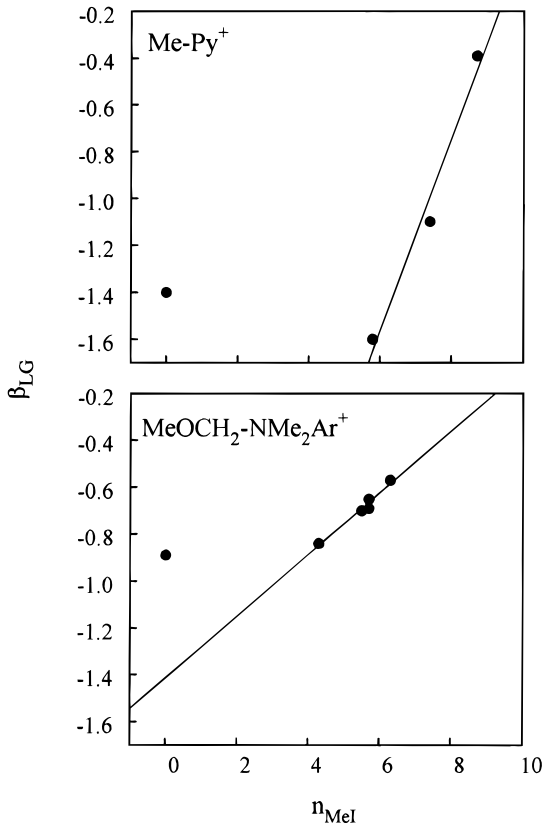

Figure 11. Cross-correlation plots for the reactions of MePy's with NaN_3 (this study), I^- (ref 27), Ph_3P (ref 28), and water (this study) and for the reactions of $MeOCH_2NMe_2Ar^+$ with HO^-, AcO^-, three primary amines, and water (ref 16). For MePy, $r = 0.986$; for $MeOCH_2NMe_2Ar^+$, $r = 0.997$.

3-cyanopyridine LG[30] (**1MeO**). The nucleophiles studied were water (Figure 12 for the contour plots; the full surface is shown in Figure S1, supporting information), N_3^-, I^- (Figure 13 for the contour plots; the full surface is shown in Figure S2, supporting information), and Me_3P, the latter used rather than Ph_3P for computational simplicity. While a full report will be published elsewhere with data for the benzyl systems and dimethylaniline LGs, the results of the initial part of the study suggest an answer to this apparent dilemma.

The computed $\Delta H^{\ddagger}$ and ΔH_R values for the reaction of **1Me** and **1MeO** with all nucleophiles correlate very well (Figure 14). The slope is smaller for **1MeO** than for **1Me**, consistent with stabilization of the activated complex by resonance.[31] In terms of the energies involved, these are perfectly well-behaved systems that follow the rate−equilibrium criterion of the Hammond−Leffler postulate.[32]

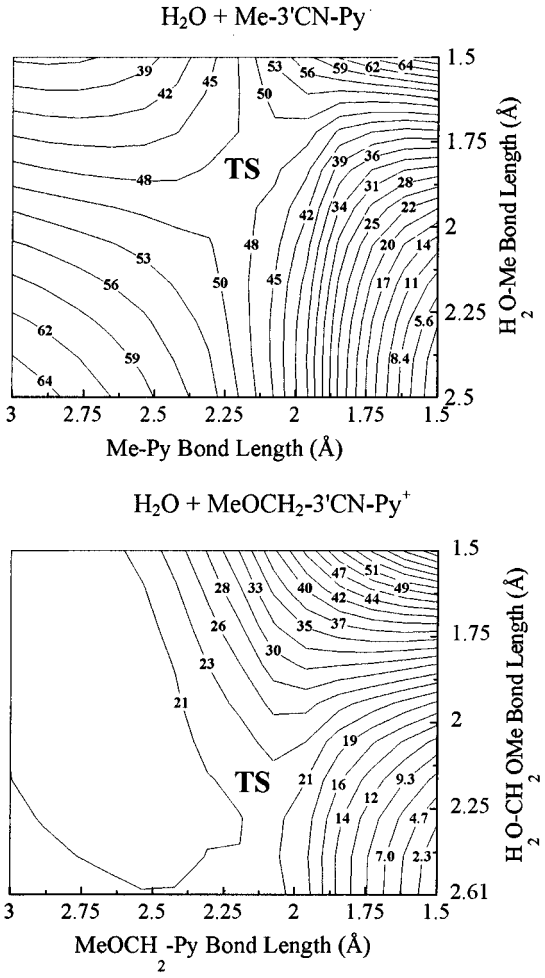

Figure 12. Contour plots of the AM1 reaction surface for the reaction of **1Me** and **1MeO** with water. The reaction begins in the lower right-hand corner. The relative energies (in kcal/mol) are given on the contour lines. The C−Py bond lengths are the same, but the C−O bond lengths are very different. Note that the surface for the $MeOCH_2$− substrate is very similar to the PM3 surface calculated for the inversion water reaction of β-nicotinamide riboside (ref 6).

Pross[22] has argued that the Brønsted parameter has no relation to charge development for MeX substrates, which have only reactant and product canonical forms that can mix to give the activated complex, but may be a relative measure of charge development in stabilized systems such as $MeOCH_2X$, in which a third canonical form involving $MeO{=}CH_2^+$ can mix into the activated

(29) Reaction surfaces were computed in AM1 (Dewar, M. J. S.; Zoebisch, E. G.; Healy, E. F.; Stewart, J. J. P. *J. Am. Chem. Soc.* **1985**, *107*, 3902−3909) using the reaction coordinate method. Enthalpies of formation (ΔH_f) for various structures were computed by varying either the Nu or LG bond length with the other held constant; for the negative Nu, the reaction coordinate was constrained to a torsional angle of 180°. The relative enthalpies for bond cleavage were obtained by subtracting the ΔH_f of the initial complex formed between substrate and Nu. After the TS had been located approximately on the surface, intermediate structures were refined until a structure was obtained that gave a single negative first normal mode on vibrational analysis (McIver, J. W., Jr.; Komornicki, A.. *Chem. Phys. Lett.* **1971**, *10*, 303−306). Enthalpies of reaction (ΔH_R) were calculated from the ΔH_f of the separated reactants and products. ΔH_R computed in PM3 (Stewart, J. J. P. *J. Comput. Chem.* **1989**, *10*, 209−220; 221−264) had different values for each structure, but the trends found in AM1 were the same. The values of E_{HOMO} and E_{LUMO} in AM1 and PM3 were very similar, however, and showed the same trends.

(30) The pyridine LG was used for consistency and computational simplicity. The pK_a's of 3-CN-pyridine (1.45) and *N*,*N*-dimethyl-3-nitroaniline (2.65) are in the same range, and ΔH_R values and HOMO-LUMO gaps for the model reactions, which are thermodynamic measures of reactivity, for both LGs correlate excellently ($r > 0.999\,99$) between the series. The plots of ΔH_R vs $E_{LUMO} - E_{HOMO}$ for the aniline LG for either the Me or $MeOCH_2$ substrate are the same as found for the pyridine LG (Figures 17 and 18). (These plots are given as supporting information.) These correlations show that the pyridine can be used for direct comparison with the experimental data. The rates for the reactions will be different because of steric and solvation factors, however.

(31) This effect is opposite that predicted by Dewar and Dougherty (Dewar, M. J. S.; Dougherty, R. C. *The PMO Theory of Organic Chemistry;* Plenum: New York, 1975; pp 262−263) on the basis of an analysis of the orbital interactions of the Nu and MeO MOs in the activated complex. The solution data are in agreement with our calculations; extrapolation of the Knier−Jencks data for water reaction of the *m*-nitrodimethylaniline substrate shows that it reacts 4800-fold faster than the unstabilized **1Me** at 80 °C.

(32) (a) Hammond, G. S. *J. Am. Chem. Soc.* **1955**, *77*, 334−338. (b) Leffler, J. E. *The Reactive Intermediates of Organic Chemistry*; Interscience: New York, 1956.

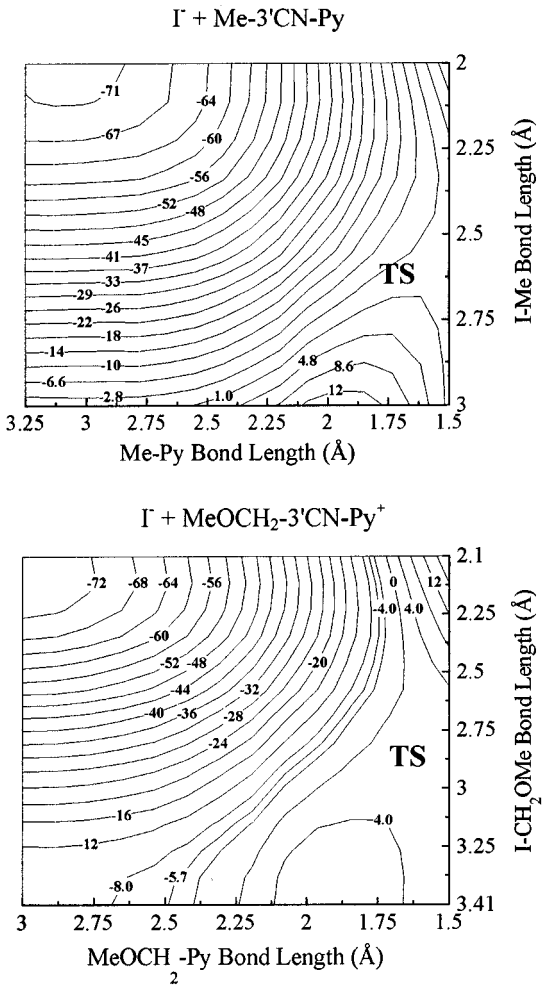

Figure 13. Contour plots of the AM1 reaction surface for the reaction of **1Me** and **1MeO** with I^-. The reaction begins in the lower right-hand corner. The relative energies (in kcal/mol) are given on the contour lines. The C−Py bond lengths are essentially the same, and the "early" C−I bond lengths have a bond order of ~0.3. The same general shape and pattern was found for N_3^- and Me_3P. Note that while the second-order rate constants for the N_3^- and I^- reaction of the (methoxymethyl)dimethylanilinium ion substrates in water are essentially the same (ref 16), the second-order rate constants for the reaction of methylpyridinium ions with iodide in acetonitrile (ref 24) are significantly lower than the rates for the NaN_3 reaction in water (this study).

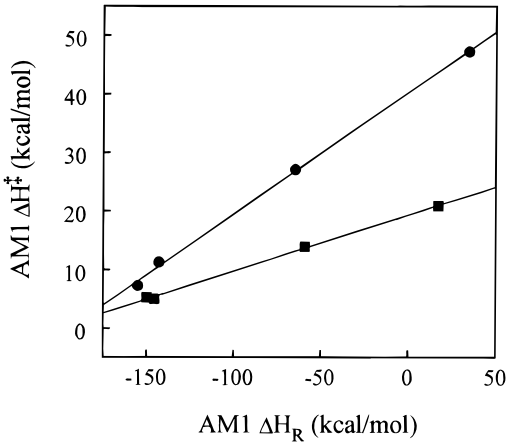

Figure 14. Rate−equilibrium AM1 enthalpy correlations for **1Me** (●) and **1MeO** (■); the slopes are 0.21 (r = 0.999) and 0.10 (r = 0.999), respectively. Left to right the points are for I^-, N_3^-, Me_3P, and water.

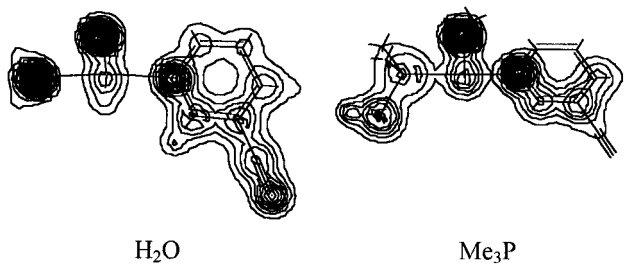

Figure 15. Charge density plots for the reaction of **1MeO** with water and Me_3P. There is a large electrostatic repulsion between the incoming water and the MeO that is not present in the reaction with Me_3P.

complex. While $\Delta H^{\ddagger}$ and ΔH_R are lower for **1MeO**, presumably because of the resonance interaction, neither **1Me** nor **1MeO** shows any discernible pattern in the change in charge at the reaction center (Δq) between the initial and activated complexes for any Nu. For instance, for **1Me** Δq = 0.09, 0.22, 0.158, and 0.310 for I^-, N_3^-, Me_3P, and water, respectively, values that do not correlate with any computed energy.

The geometries of the activated complexes, however, are anomalous. For the reactions of **1Me** and **1MeO** with N_3^-, I^-, and Me_3P, the TS occurs at a C−Py bond length of ~1.75 Å ("early") and an "early" or intermediate C−Nu bond length. For the water reaction, however, the TS occurs at C−O bond lengths of ~1.8 Å for **1Me** ("late" for the Nu) and ~2.25 Å for **1MeO** ("early" for the Nu), which is consistent with resonance stabilization of the TS for **1MeO**. The C−Py bond lengths are ~2.15 Å ("late" for the LG) in both cases. Thus, while the rates are different, reflected in the different values of $\Delta H^{\ddagger}$ for each reaction, the structures of the activated complexes are the same for I^-, N_3^-, and Me_3P displacement, but not for the water reactions. In neither system do the bond lengths to the Nu or LG correlate with the β_{LG}.

The difference between the O−C TS bond lengths for **1Me** and **1MeO** is probably the result of charge repulsion in the activated complex for **1MeO**. As the activated complex is formed in both substrates, a net positive charge builds up on the water oxygen. A repulsive interaction with the positively charged pyridine nitrogen would be partially shielded by the methyl in both. In **1Me**, there is no other interaction; in **1MeO**, however, as the resonance interaction develops and positive charge is building up on the MeO oxygen, electrostatic repulsion between the two oxygens would cause an earlier TS (Figure 15). The greater stabilization afforded by the resonance interaction is sufficient to overcome the energy of this repulsive term. This interaction is avoided in the phosphine TS because of either or both the greater polarizability of P or because of hyperconjugation that places the bulk of the charge on the phosphine methyls; accordingly, the reaction surface for this neutral Nu closely resembles that for the negative Nu's.

The reason for the longer length of the C−N bond in the water reaction is apparent from an examination of the frontier MOs for the different Nu's. Upon formation of the initial complex, the HOMO of the entire complex remains localized on the Nu for all complexes except the two water structures, in which the HOMO is localized on the LG (Figure 16). The LUMO of the initial complex is localized on the water. Both the HOMO−LUMO gap (E_{LUMO} for the substrate − E_{HOMO} for the Nu, Figure 17) and the E_{HOMO} for the activated complex (Figure 18) show the same relationship found in the cross-correlation plots (Figure 11). These FMO localizations are the result of

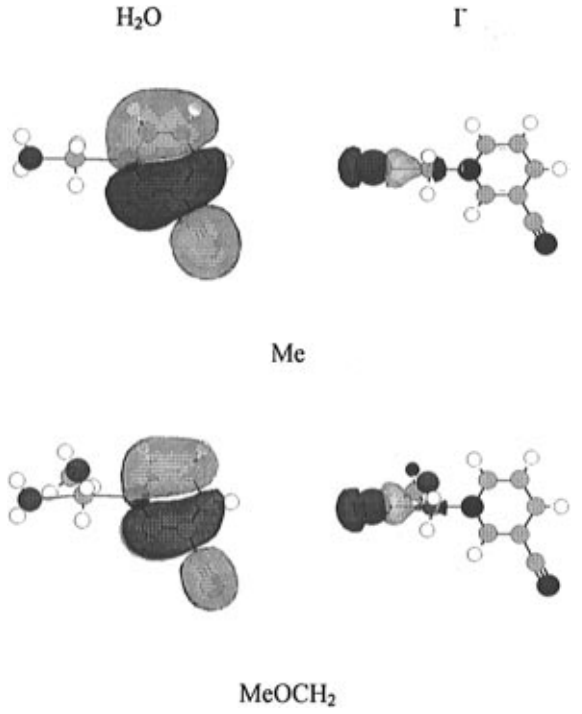

Figure 16. HOMOs in the activated complexes for the reaction of water and I^- with **1Me** and **1MeO**. The HOMO is localized on the LG for the water reaction and on the Nu for the iodide reaction; N_3^- and Me_3P show essentially the same pattern as I^-. This difference appears to be related to the position of the activated complex on the reaction surface.

the fact that the activated complexes for the water reactions are close in structure to the initial complexes for the back reactions, pyridine displacement of water from ^+H_2OMe or $^+H_2OCH_2OMe$. Thus, both charge repulsion in the activated complex (for **1MeO**) and the position of the TS on the potential energy surface (for **1Me** and **1MeO**) contribute to the anomalous bond lengths in the activated complexes.

With a different potential carbenium ion in the substrate, the picture is also complicated and shows that β_{LG} values alone are not a good criterion with which to assess mechanism. β_{LG} values of −1.11 and −0.91 have been reported for the hydrolysis (100 °C) and NAD^+ gylcosyl hydrolase-catalyzed cleavage (37 °C), respectively, of NAD^+ analogs with different pyridine LGs,[4] and Sinnott[33] reported a β_{LG} value of −1.29 for the hydrolysis of β-D-galactopyranosylpyridinium ions. While these values are in the same high ranges as the clean concerted displacement reactions for the methyl and benzyl substrates, there are other results that suggest the ribosyl and glycosyl reactions are dissociative. Hydrolysis reactions for all the glycosyl-, and ribosyl-, and arabinosylpyridinium ions have high, positive values of $\Delta S^{\ddagger}$.[33] Ta-Shma and Oppenheimer[34] found that that N_3^- traps the solvent-separated NAD^+ IDC, and in a recent study, Bennet[35] found that products from the hydrolysis of deoxyglucosylpyridinium ions arise from trapping of the same intermediate. These values are consistent with a "loose" activated complex for a unimolecular process through a stable oxocarbenium ion intermediate or IDC. It is clear

(33) Hosie, L.; Marshall, P. J.; Sinnott, M. L. *J. Chem. Soc., Perkin Trans. 2*, **1984**, 1121−1131. For earlier work, see: Capon, B. *Chem. Rev.* **1969,** *69*, 407−498. Cordes, E. H.; Bull, H. G. *Chem. Rev.* **1973,** *73*, 581−603.

(34) Ta-Shma, R.; Oppenheimer, N. J., Manuscript in preparation.

(35) Huang, X.; Surry, C.; Hiebert, T.; Bennet, A. J. *J. Am. Chem. Soc.* **1995**, *117*, 10614−10621.

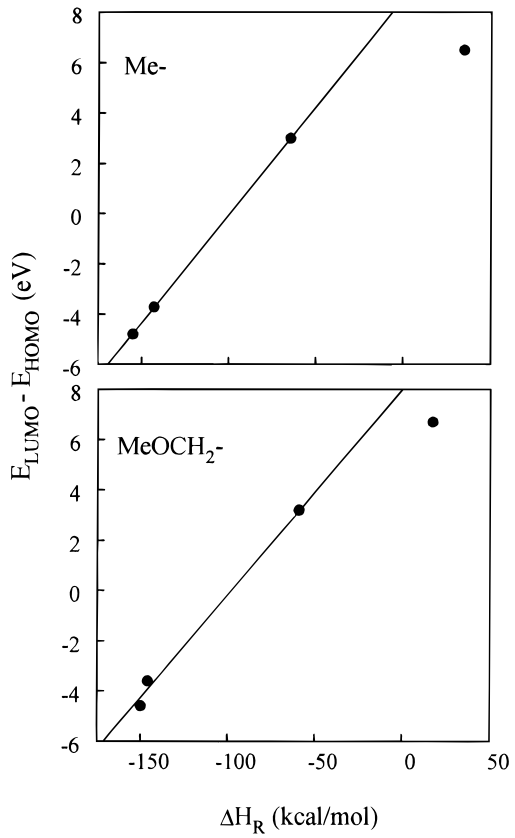

Figure 17. Plots of the energy of the HOMO−LUMO gap vs ΔH_R, a measure of the thermodynamic characteristics of the reaction that shows the same anomaly as the cross-correlation plots (Figure 11). Left to right the points are for I^-, N_3^-, Me_3P, and water. The slopes are essentially the same, 0.086 (r = 0.999 97) for **1Me** and 0.082 (r = 0.9969) for **1MeO**.

from these data that the Brønsted value is independent of the mechanism of substitution with the same LG class, with comparable or larger values obtained for the S_N2 reactions of substrates that do (benzyls) or do not (methyls) contain potentially stable carbenium ions.

What is so startling about all the above results is the lack of a clear predictive pattern between the Brønsted coefficient and mechanism in series with similar LGs in terms of charge and pK_a. The computational results suggest that there is no single source of the Brønsted coefficients, the values of which appear to depend on the interplay of several factors, and that they depend on the system. Attempting to compare results between series of different structures emphasizes Hammond's specific warning[32a] that *free energies or their relations* may not correlate with the *potential energy surfaces* upon which his postulate is based and that the postulate should not be applied to systems in which the reactants and activated complexes are separated by large energies. As Arnett and Reich[27] point out, Hammond[32a] explicitly excluded use of the postulate to evaluate S_N2 reactions of this type.

The Possibility of a Preassociation Mechanism. In our study of the nucleophilic substitution reactions of (4-methoxybenzyl)dimethylsulfonium chloride,[10] we found kinetic evidence for the simultaneous operation of three substitution mechanisms: a stepwise mechanism with capture of the carbenium ion by nucleophile and solvent, a simple concerted displacement reaction—the Hughes-Ingold S_N2 mechanism—and a preassociated-concerted mechanism in which a negative—but not a neutral—nucleophile and positively charged substrate

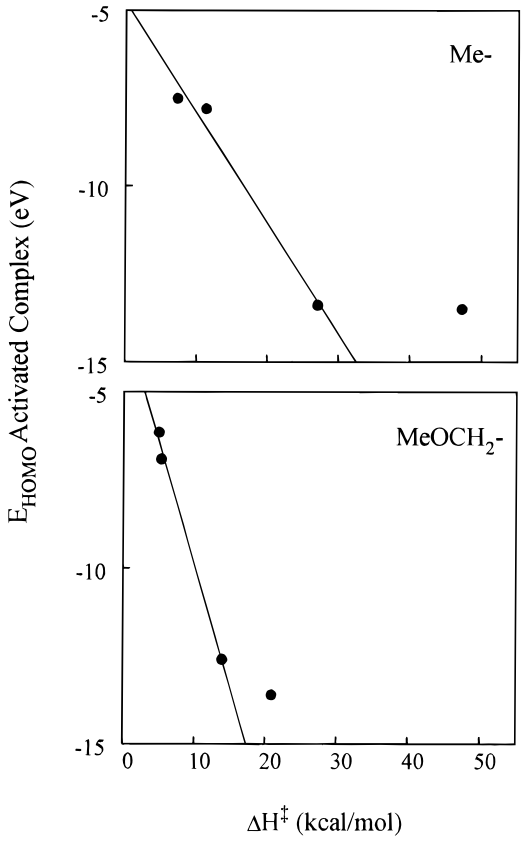

Figure 18. Plots of the energy of the HOMO for the activated complex vs $\Delta H^{\ddagger}$, a measure of the kinetic characteristics of the reaction that shows the same anomaly as the cross-correlation plots (Figure 11). Left to right the points are for I^-, N_3^-, Me_3P, and water. The slopes are different because of the differences in $\Delta H^{\ddagger}$.

preform an ion pair $Nu:^{-}\cdot RX^{+}$ that is an *intermediate* on the reaction coordinate. In the presence of exogenous salt added to control ionic strength, formation of the nucleophile−substrate ion pair is in competition with formation of the salt−substrate ion pair and is of much less importance at lower than at higher [Nu]. In the presence of added nucleophile only, however, the two concerted mechanisms can compete efficiently. These effects could be seen in plots of k_{obsd} vs [Nu]; in the presence of exogenous salt, this plot was linear over most of the range of [Nu] (up to 5 M NaN_3). With no added salt, however, the plot exhibited a break at low [Nu] that signaled the switch from Hughes−Ingold S_N2 to preassociated-concerted mechanisms, with some diminution in the rate of the unimolecular process related to the total ionic strength of the solution. While the kinetic profile was clear, the different mechanisms were established with certainty by fitting the rate constants for each process to equations that relate the product ratio [RNu]/[ROH] to the rate constants for the various processes.[10]

In principle, there is no reason why these pyridinium ion substrates should not have the same mix of mechanisms. As shown in Figure 19, the rate constants obtained for the reaction of **1a** with NaN_3 alone in the range 0−1.7 M NaN_3 describe a smooth curve with rates greater than found under constant ionic strength. If there is a break in this curve, it is much too small to detect accurately, unlike the results for the sulfonium substrate. In addition, the points seem to fit fairly well rate constants calculated with a Winstein−Fainberg[36] *b* value of −0.41 (x's and line, Figure 19), which suggests that the rate constants in the absence of added salt

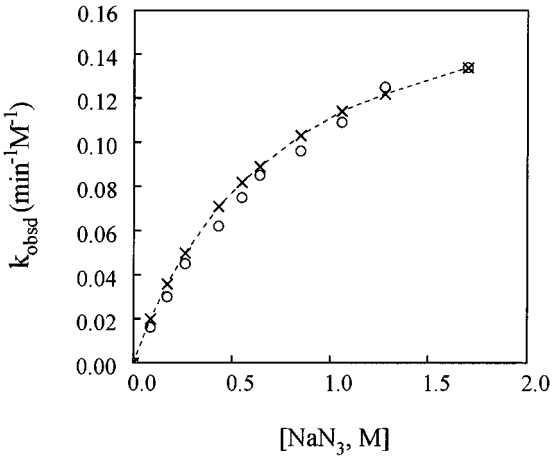

Figure 19. Plots of k_{obsd} vs [NaN_3] with no control of ionic strength by addition of exogenous salt. The circles are the measured values, the ×'s values computed using a Winstein−Fainberg *b* value of −0.4 determined from second-order rate constants obtained under conditions of ionic strength. The line through the ×'s has no physical meaning, but is there only to guide the eye. The experimentally determined values appear to match, within error, the computed line.

merely reflect the effect of ionic strength on rate and not a preassociation mechanism. A negative primary salt effect is evident even under conditions of constant ionic strength, as shown by the slight curvature of the plot of k_{obsd} vs [NaN_3] at $\mu = 1.7$ (see Figure 1; similar curvature is found in a plot of data for reaction at $\mu = 4$), which is consistent with this view. In any case, because there is no ROH formed for **1a**, it is not possible to evaluate this possibility with the definitive product ratio test used in the sulfonium ion work.[10]

If there is no preassociation mechanism at work here, it is not surprising. Pyridinium ions are well-known to bind anions to the face of the pyridine ring to form charge-transfer complexes, the basis of Kosower's Z-scale for solvent polarity.[37] In these complexes, the nucleophile would be bound nonproductively with regard to the necessary geometry for the displacement reaction. In addition, the charge on the ring is reduced by formation of the charge-transfer complex, which makes the pyridine a worse LG. None of these physical impediments is present in $Nu^{-}\cdot RSMe_2^{+}$ ion pairs.

The Effect of Solvent. Our results for the pyridinium and sulfonium ions[10] are in accord with the suggestion of Arnett and Reich[24] that the effects of solvation of the LG at the TS are important determinants of reactivity. On the basis of the pK_a's of the LGs, it would be expected that the dimethylsulfoniums ($pK_a = -6$) would react much faster than the pyridinium ions ($pK_a = 1.45-5.25$). There is a difference in $\Delta H^{\ddagger}$ between the series, with $\Delta H^{\ddagger} \sim 22$ kcal/mol for the sulfonium ions[10] and ~16 kcal/mol for the pyridinium ions (Table 2), which reflects the difference in pK_a and/or the stability of the substrate as a Lewis complex (sulfonium ions: soft−soft; pyridinium ions: soft−intermediate for the carbenium ion−LG bond). Despite these differences, the second-order rate constants at 80 °C are the same within

(36) Fainberg, A. H.; Winstein, S. *J. Am. Chem. Soc.* **1956**, *78*, 2763−2767. In this instance we used the equation $k = k_o(1 - b\Delta[salt])$, where Δ[salt] is the difference for reaction at two different ionic strengths. Values of k_{calc} obtained are second-order rate constants at the ionic strength of the nucleophile alone; computed k_{obsd} are then k_{calc}[Nu].

(37) Kosower, E. M. *An Introduction to Physical Organic Chemistry*; Wiley: New York, 1968; pp 295−304.

a factor of 2. Thus, other factors must be important, including the effect of solvent.

The values of $\Delta G^{\ddagger}$ (25.2 kcal/mol) for the reaction of **1a** and the corresponding dimethylsulfonium with NaN_3 are the same, but the value of $\Delta\Delta S^{\ddagger}$ is −15 gibbs/mol.[10] The enthalpy and entropy required to desolvate the nucleophile and the translational entropy loss in bringing the nucleophile and substrate together will be the same for both substrates. For charged substrates, the ground state and activated complexes both bear a full formal positive charge, and only small adjustments in solvation at the reaction center are needed as the transition state is achieved with a subsequent small loss of solvation entropy. In fact, solvolysis of (4-methoxybenzyl)dimethylsulfonium ion is not very sensitive to solvent polarity and exhibits a low *m* value.[11] The substantial difference in $\Delta S^{\ddagger}$ must reflect the large, unfavorable change in solvation entropy of introducing the hydrophilic 3-cyanopyridine into bulk solvent at the TS and the minor entropic effects of introducing the hydrophobic SMe_2 into the cavities or interstitial spaces in bulk solvent. Substantial differences between $\Delta S^{\ddagger}$ for the S_N1 solvolysis of (4-methoxybenzyl)dimethylsulfonium in H_2O ($\Delta S^{\ddagger}$ = 14.5 gibbs/mol)[11] and in D_2O ($\Delta S^{\ddagger}$ = 7 gibbs/mol)[10] are also consistent with this expression of the hydrophobic effect on kinetics. Values of $\Delta S°$ are slightly more negative for the introduction of noble gases and simple hydrocarbons into D_2O than into H_2O,[38] which is the result of the slightly (5−7%) stronger deuterium bonds in D_2O. Thus, it is possible that **1a** does not undergo an S_N1 reaction because of the unfavorable entropy of solvation of the LG, but this is an unproven speculation based on a rather large extrapolation.

Difference between the Solution and Enzyme-Catalyzed Cleavage of the Nicotinamide−Ribosyl Bond in NAD$^+$. Handlon et al.[3] have shown recently that the Taft plots for hydrolysis (log k_{obsd}) and enzyme-catalyzed (log V_{max}) cleavage of a series of 2′-substituted β-nicotinamide ribosides and the corresponding 2′-substituted NAD^+ analogs give high ρ_I values (−6.9 and −9.5, respectively). The higher value for the enzyme reaction may reflect different intermediates formed in dissociative reactions, a solvent-separated IDC in solution and an oxocarbenium ion bound to the active site of the enzyme. On the basis of high β_{LG} values and the difference in partitioning of MeOH and water in the products of solvolysis ($k_{MeOH}/k_{HOH} \sim 2$) and the enzyme-catalyzed reaction ($k_{MeOH}/k_{HOH} \sim 100$), Schuber[4] argued that the enzyme-bound intermediate was a stable ribosyloxocarbenium ion. We reported recently[8,14] that in the gas phase the arabinosyloxocarbenium ion is more stable than the (4-methoxybenzyl)carbenium ion. All of these results are consistent with a recent conclusion of Richard et al.[39] that the intermediate formed by β-galactosidase-catalyzed hydrolysis of galactosides is a stable oxocarbenium ion in the active site. The results are not consistent with a displacement mechanism involving an active site nucleophile with formation a ribosyl−acyl intermediate. There is a large rate difference, however, between the solution and enzyme reactions for NAD^+ analogs: at the same temperature and pH, the enzyme-catalyzed reaction is ca. 10^4 faster (in V_{max}) than the solution reaction.

How *does* an enzyme "catalyze" an S_N1 reaction? Binding of NAD^+ in the enzyme active site should effectively desolvate the pyridinium ion, and all other things being equal, the difference in rate for bond cleavage may be related to removal in the enzyme active site of the retarding effects of an unfavorable $\Delta S^{\ddagger}$ caused by solvation of the LG. The $\Delta\Delta S^{\ddagger}$ of −15 gibbs/mol between **1a** and the corresponding dimethylsulfonium ion—between extensive solvent rearrangement for the pyridinium ion and essentially no solvent reorganization for the dimethylsulfonium ion—is worth ca. 3×10^3 in relative rate, within a factor of 10 of the difference between the solution and enzyme-catalyzed rates for NAD^+ analogs. Thus, in this system enzyme "catalysis" of bond cleavage may be a solvent effect. This may not be the entire story, however, because several 2′-substituted arabio NAD^+ analogs are quite good inhibitors of the enzyme,[40] which is not consistent with a simple desolvation argument. Reasons for the difference between the ribo and arabino series are under active investigation.

The presence of a stable oxocarbenium ion intermediate in the enzyme active site, proposed earlier by Schuber[4] for glycosylhydrolases and confirmed by the recent results of Richard[39] for β-galactosidase, challenges the contention[18] that ribosyl- and glycosyloxocarbenium ions cannot exist as intermediates in enzymes such as lysozyme. We argued elsewhere[8] that it is not always wise to assign mechanism based on an extrapolation from the gas to solution phase; these results suggest that extrapolations from solution to enzymes must be done with caution.

Acknowledgment. Supported in part by NIH Grant No. GM-22982 (N.J.O), a Biotechnology Grant from the State of California (N.J.O., N.B.), and a Research Award from the UCSF Graduate Division (N.B.). The UCSF Magnetic Resonance Laboratory is supported in part by grants from the NSF (DMB 8406826) and the NIH (RR-01668 and RR-4789). Funds for the purchase and support of the tandem spectrometer in the UCSF Mass Spectrometry Facility (A. L. Burlingame, Director) were provided by a grant from the Division of Research Resources (RR 01614) of the NIH and a grant from the NSF (DIR 8700766); we thank David Maltby for obtaining the LSIMS spectra.

Supporting Information Available: Full potential energy surfaces for the water and iodide displacement reactions on methyl- and (methoxymethyl)pyridinium ions and various correlation plots that show the correspondence between pyridine and dimethylaniline leaving groups (7 pages). This material is contained in libraries on microfiche, immediately follows this article in the microfilm version of the journal, and can be ordered from the ACS; see any current masthead page for ordering information.

JO960729J

(38) Ben-Naim, A. *Solvation Thermodynamics*; Plenum Press: New York, 1987; pp 75−77.

(39) Richard, J. P.; Westerfeld, J. G.; Lin, S.; Beard, J. *Biochemistry* **1995**, *34*, 11713−11724.

(40) Schuber, F.; Oppenheimer, N. J. Unpublished results.